

ParaDIAG: Parallel-in-Time Algorithms Based on the *Diagonalization* Technique

Martin J. Gander^a Jun Liu^b Shu-Lin Wu^c Xiaoqiang Yue^d Tao Zhou^e

^a*Section of Mathematics, University of Geneva, CH-1211 Geneva, Switzerland*

E-mail: martin.gander@unige.ch

^b*Department of Mathematics and Statistics,*

Southern Illinois University Edwardsville, Edwardsville, IL 62026, USA

E-mail: juliu@siue.edu

^c*School of Mathematics and Statistics, Northeast Normal University,*

Changchun 130024, China

E-mail: wushulin84@hotmail.com

^d*School of Mathematics and Computational Science, Xiangtan University,*

Xiangtan 411105, China

E-mail: yuexq@xtu.edu.cn

^e*Institute of Computational Mathematics and Scientific/Engineering Computing,*

AMSS, the Chinese Academy of Sciences, Beijing, China

Email: tzhou@lsec.cc.ac.cn

Contents

1 Basic idea of ParaDIAG	2
2 ParaDIAG for Linear Advection-Diffusion Problems	3
2.1 ParaDIAG-I	4
2.2 ParaDIAG-II	5
2.2.1 ParaDIAG-II – Waveform Relaxation (WR) Variant	5
2.2.2 ParaDIAG-II – Parareal Variant	9
3 ParaDIAG-II – Krylov Variant (for wave equations)	12
4 ParaDIAG-II – Krylov Variant (for optimal control of the wave equation)	13

Abstract

In 2008, Maday and Rønquist introduced an interesting new approach for the direct parallel-in-time (PinT) solution of time-dependent PDEs. The idea is to diagonalize the time stepping matrix, keeping the matrices for the space discretization unchanged, and then to solve all time steps in parallel. Since then, several variants appeared, and we call these closely related algorithms *ParaDIAG* algorithms. ParaDIAG algorithms in the literature can be classified into two groups:

- ParaDIAG-I: direct standalone solvers,
- ParaDIAG-II: iterative solvers,

We will explain the basic features of each group in this note. To have concrete examples, we will introduce ParaDIAG-I and ParaDIAG-II for the advection-diffusion equation. We will also introduce ParaDIAG-II for the wave equation and an optimal control problem for the wave equation. We could have used the advection-diffusion equation as well to illustrate ParaDIAG-II, but wave equations are known to cause problems for certain PinT algorithms and thus constitute an especially interesting example for which

ParaDIAG algorithms were tested. We show the main known theoretical results in each case, and also provide Matlab codes for testing. The goal of the Matlab codes is to help the interested reader understand the key features of the ParaDIAG algorithms, without intention to be highly tuned for efficiency and/or low memory use.

We also provide speedup measurements of ParaDIAG algorithms for a 2D linear advection-diffusion equation. These results are obtained on the Tianhe-1 supercomputer in China, which is a multi-array, configurable and cooperative parallel system, and we compare these results to the performance of parareal and MGRiT, two widely used PinT algorithms. In a forthcoming update of this note, we will provide more material on ParaDIAG algorithms, in particular further Matlab codes and parallel computing results, also for more realistic applications.

Matlab codes for re-producing the numerical results of the current work can be downloaded via: <http://parallel-in-time.org/codes/index.html>.

1 Basic idea of ParaDIAG

We start with a basic introduction to ParaDIAG algorithms. Suppose we need to solve in parallel the system of ODEs $M\dot{U}(t) + KU(t) = f(t)$ with initial value $U(0) = U_0$ arising from the semi-discretization of a time-dependent PDE, where $M, K \in \mathbb{C}^{N_x \times N_x}$. For finite element discretizations, M is the mass matrix and K is the stiffness matrix. For finite difference discretizations, $M = I_x$ is just an identity matrix. The classical approach for solving such systems of ODEs is to apply a time-integrator, and then solve the resulting difference equation step-by-step in time. Instead, ParaDIAG tries to solve these difference equations *all-at-once*. For linear multi-step methods, the all-at-once system is of the form

$$\mathbf{A}\mathbf{u} = \mathbf{b}, \quad \mathbf{A} := B_1 \otimes M + B_2 \otimes K, \quad (1.1)$$

where $B_1, B_2 \in \mathbb{R}^{N_t \times N_t}$ are Toeplitz matrices specified by the time-integrator and N_t is the number of time steps¹. All ParaDIAG algorithms focus on treating the matrices B_1 and B_2 , while keeping M and K unchanged. There are mainly two approaches: first, using different step sizes $\{\Delta t_n\}$, e.g., a geometrically increasing sequence $\Delta t_n = \Delta t_1 \tau^{n-1}$ with $\tau > 1$, which makes the time-discretization matrices diagonalizable. This yields ParaDIAG algorithms which are direct solvers in the ParaDIAG-I group [5, 7, 12].

The second treatment is to use a uniform step size Δt and solve the all-at-once system (1.1) iteratively, which leads to ParaDIAG algorithms in the ParaDIAG-II group. There are several variants, but the common point is to introduce the α -circulant block matrix

$$\mathbf{P}_\alpha := C_1^{(\alpha)} \otimes M + C_2^{(\alpha)} \otimes K, \quad (1.2)$$

where $C_1^{(\alpha)}$ and $C_2^{(\alpha)}$ are Strang type α -circulant matrices constructed from B_1 and B_2 , and $\alpha \in (0, 1]$ is a free parameter. One can then either solve (1.1) via the stationary iteration [18]

$$\mathbf{P}_\alpha \mathbf{u}^k = (\mathbf{P}_\alpha - \mathbf{A}) \mathbf{u}^{k-1} + \mathbf{b}, \quad (1.3)$$

where $k \geq 1$ is the iteration index, or via Krylov subspace methods (e.g., GMRES, MINRES) by solving the preconditioned system [13]

$$\mathbf{P}_\alpha^{-1} \mathbf{A} \mathbf{u} = \mathbf{P}_\alpha^{-1} \mathbf{b}, \quad (1.4)$$

which is nothing else than the stationary iteration (1.3) written at its fixed point, i.e. at convergence.

The algorithms proposed in [15] and [8] are essentially ParaDIAG-II algorithms as well, but they are derived from a different point of view. For example, in [8] the authors introduced a Waveform Relaxation (WR) iteration $M\dot{U}^k(t) + KU^k(t) = f(t)$, $U^k(0) = \alpha(U^k(T) - U^{k-1}(T)) + U_0$, and after a time-discretization one can show that at each iteration the all-at-once system is $\mathbf{P}_\alpha \mathbf{u}^k = \mathbf{b}^{k-1}$, where $\mathbf{b}^{k-1} = (\mathbf{P}_\alpha - \mathbf{A}) \mathbf{u}^{k-1} + \mathbf{b}$. The algorithm in [15] can be understood similarly.

For each variant of ParaDIAG-II we need to compute $\mathbf{P}_\alpha^{-1} \mathbf{r}$ with \mathbf{r} being an input vector. The reason for using \mathbf{P}_α is twofold: first, since $C_1^{(\alpha)}$ and $C_2^{(\alpha)}$ are Strang type α -circulant matrices constructed from the Toeplitz matrices B_1 and B_2 , it naturally holds that \mathbf{P}_α converges to \mathbf{A} as α goes to zero. This implies that by using a relatively small α , the ParaDIAG-II algorithms converge rapidly. The second point lies in the fact that $C_1^{(\alpha)}$ and $C_2^{(\alpha)}$ can be diagonalized simultaneously, as is shown in the following Lemma.

¹For Runge-Kutta methods, the all-at-once system is different and will be treated in a forthcoming update of this note.

Lemma 1 (see [3]) Let $\mathbb{F} = \frac{1}{\sqrt{N_t}} [\omega^{(l_1-1)(l_2-1)}]_{l_1, l_2=1}^{N_t}$ (with $i = \sqrt{-1}$ and $\omega = e^{\frac{2\pi i}{N_t}}$) be the discrete Fourier matrix and define for any given parameter $\alpha \in (0, 1]$ the diagonal matrix

$$\Gamma_\alpha = \begin{bmatrix} 1 & & & \\ & \alpha^{\frac{1}{N_t}} & & \\ & & \ddots & \\ & & & \alpha^{\frac{N_t-1}{N_t}} \end{bmatrix}.$$

Then the two α -circulant matrices $C_1^{(\alpha)}, C_2^{(\alpha)} \in \mathbb{C}^{N_t \times N_t}$ can be simultaneously diagonalized as

$$C_j^{(\alpha)} = V D_j V^{-1}, \quad D_j = \text{diag} \left(\sqrt{N_t} \mathbb{F} \Gamma_\alpha C_j^{(\alpha)}(:, 1) \right), \quad j = 1, 2,$$

where $V = \Gamma_\alpha^{-1} \mathbb{F}^*$ and $C_j^{(\alpha)}(:, 1)$ represents the first column of $C_j^{(\alpha)}$, $j = 1, 2$.

Due to the property of the Kronecker product, we can factor $\mathbf{P}_\alpha = (V \otimes I_x)(M \otimes D_1 + A \otimes D_2)(V^{-1} \otimes I_x)$ and thus we can compute $\mathbf{P}_\alpha^{-1} \mathbf{r}$ by performing the following three steps:

- Step-(a) $S_1 = (V^{-1} \otimes I_x) \mathbf{r}$,
- Step-(b) $S_{2,n} = (\lambda_{1,n} M + \lambda_{2,n} A)^{-1} S_{1,n}$, $n = 1, 2, \dots, N_t$,
- Step-(c) $\mathbf{u} = (V \otimes I_x) S_2$,

where $S_1 = (S_{1,1}^\top, \dots, S_{1,N_t}^\top)^\top$ and $S_2 = (S_{2,1}^\top, \dots, S_{2,N_t}^\top)^\top$. Since V and V^{-1} are given by FFT techniques, Step-(a) and Step-(c) can be computed efficiently with $O(N_x N_t \log N_t)$ operations. Step-(b) can be computed in parallel since all linear systems are completely independent from each other at different time points. These three steps represent the key steps of ParaDIAG algorithms and will appear frequently in this note, although the details differ in the various cases.

For nonlinear problems $M \dot{U} + f(U) = 0$ with $U(0) = U_0$, the basic idea for applying ParaDIAG algorithms is as follows: for linear multi-step methods, the non-linear all-at-once system is

$$(B_1 \otimes M) \mathbf{u} + (B_2 \otimes I_x) F(\mathbf{u}) = \mathbf{b}, \quad (1.6)$$

where $F(\mathbf{u}) = (f^\top(U_1), \dots, f^\top(U_{N_t}))^\top$. The Jacobian matrix of (1.6) is

$$B_1 \otimes M + (B_2 \otimes I_x) \nabla F(\mathbf{u}), \quad (1.7)$$

where $\nabla F(\mathbf{u}) = \text{blkdiag}(\nabla f(U_1), \dots, \nabla f(U_{N_t}))$. To apply ParaDIAG, we approximate the Jacobian matrix (1.7) by

$$\mathbf{P}_\alpha(\mathbf{u}) := C_1^{(\alpha)} \otimes M + C_2^{(\alpha)} \otimes \overline{\nabla f}(\mathbf{u}),$$

where $\overline{\nabla f}(\mathbf{u})$ is constructed from the N_t values $\{U_n\}$ by some *averaging* [6], e.g., $\overline{\nabla f}(\mathbf{u}) = \frac{1}{N_t} \sum_{n=1}^{N_t} \nabla f(U_n)$ or $\overline{\nabla f}(\mathbf{u}) = \nabla f(\frac{1}{N_t} \sum_{n=1}^{N_t} U_n)$. Then, we can solve (1.6) by the following simplified Newton iteration:

$$\mathbf{P}_\alpha(\mathbf{u}^{k-1}) \Delta \mathbf{u}^{k-1} = -((B_1 \otimes M) \mathbf{u}^{k-1} + (B_2 \otimes I_x) F(\mathbf{u}^{k-1}) - \mathbf{b}), \quad \mathbf{u}^k = \mathbf{u}^{k-1} + \Delta \mathbf{u}^{k-1}, \quad (1.8)$$

where for each iteration the increment $\Delta \mathbf{u}^{k-1}$ can be obtained using a ParaDIAG algorithm performing the three steps in (1.5). If we use different step sizes as in [6], then B_1 and B_2 are already diagonalizable, and we can replace \mathbf{P}_α by $B_1 \otimes M + (B_2 \otimes I_x) \overline{\nabla f}(\mathbf{u}^{k-1})$ in (1.8).

In practice, the ParaDIAG algorithms can be combined with a *windowing* technique: after a certain number of time steps computed in parallel in the current time window, the computation can be restarted for the next time window in a sequential way. This permits the use of a certain adaptivity in time and space.

2 ParaDIAG for Linear Advection-Diffusion Problems

To illustrate the ParaDIAG-I and ParaDIAG-II algorithms, we now use the concrete example of the advection-diffusion equation with periodic boundary conditions²

$$\begin{cases} u_t - \nu u_{xx} + u_x = 0, & (x, t) \in (-1, 1) \times (0, T), \\ u(-1, t) = u(1, t), & t \in (0, T), \\ u(x, 0) = e^{-30x^2}, & x \in (-1, 1), \end{cases} \quad (2.1)$$

²We use periodic boundary condition make the advection dominated situation harder for PinT algorithms, see [4].

where $\nu > 0$. Using the *method of lines* and a centered finite difference scheme for the spatial derivatives, we get the system of ODEs

$$\dot{U}(t) + AU(t) = 0, \quad U(0) = U_0, \quad (2.2a)$$

where the matrix $A \in \mathbb{R}^{N_x \times N_x}$ is

$$A = \frac{\nu}{\Delta x^2} \begin{bmatrix} 2 & -1 & & -1 \\ -1 & 2 & -1 & \\ & \ddots & \ddots & \ddots & \\ & & -1 & 2 & -1 \\ -1 & & -1 & 2 & \end{bmatrix} + \frac{1}{2\Delta x} \begin{bmatrix} 0 & 1 & & -1 \\ -1 & 0 & 1 & \\ & \ddots & \ddots & \ddots & \\ & & -1 & 0 & 1 \\ 1 & & -1 & 0 & \end{bmatrix}. \quad (2.2b)$$

Here $N_x = \frac{2}{\Delta x}$, and the periodic boundary conditions cause a zero eigenvalue in the matrix A .

2.1 ParaDIAG-I

To use ParaDIAG as a direct solver, one has to use all different time steps to make the time stepping matrix diagonalizable, and one possibility is to use geometrically increasing time step sizes $\{\Delta t_n\}$ to discretize (2.2a) as proposed in [12],

$$\Delta t_n = \Delta t_1 \tau^{n-1}, \quad n \geq 1, \quad (2.3)$$

where $\tau > 1$ is free parameter and Δt_1 is the first step size. We use the linear θ -method,

$$\frac{U_{n+1} - U_n}{\Delta t_{n+1}} + A[\theta U_{n+1} + (1 - \theta)U_n] = 0, \quad n = 0, 1, \dots, N_t - 1. \quad (2.4)$$

We will only consider $\theta = 1$ and $\theta = \frac{1}{2}$, which corresponds to the Backward-Euler method and the Trapezoidal rule. For $\theta = \frac{1}{2}$, the method is also called the Crank-Nicolson scheme. The N_t difference equations (2.4) can be combined into the *all-at-once* system

$$(B_1 \otimes I_x + B_2 \otimes A) \mathbf{u} = \mathbf{b}, \quad (2.5a)$$

where $\mathbf{u} = (U_1^\top, \dots, U_{N_t}^\top)^\top$, $I_x \in \mathbb{R}^{N_x \times N_x}$ is an identity matrix and $B_1, B_2 \in \mathbb{R}^{N_t \times N_t}$ are matrices representing the time-discretization, namely

$$B_1 = \begin{bmatrix} \frac{1}{\Delta t_1} & & & \\ -\frac{1}{\Delta t_2} & \frac{1}{\Delta t_2} & & \\ & \ddots & \ddots & & \\ & & -\frac{1}{\Delta t_{N_t}} & \frac{1}{\Delta t_{N_t}} & \end{bmatrix}, \quad B_2 = \begin{bmatrix} \theta & & & \\ 1 - \theta & \theta & & \\ & \ddots & \ddots & & \\ & & 1 - \theta & \theta & \end{bmatrix}. \quad (2.5b)$$

The right hand-side \mathbf{b} is given by $\mathbf{b} = (b_1^\top, 0, \dots, 0)^\top$ with $b_1 = \left(\frac{I_x}{\Delta t_1} - (1 - \theta)A \right) U_0$.

Let $B := B_2^{-1} B_1$ and $\tilde{\mathbf{b}} := (B_2^{-1} \otimes I_x) \mathbf{b}$. Then, we can rewrite (2.5a) as

$$(B \otimes I_x + I_t \otimes A) \mathbf{u} = \tilde{\mathbf{b}}, \quad (2.6)$$

where $I_t \in \mathbb{R}^{N_t \times N_t}$ is an identity matrix. The diagonalization of B for $\theta = 1$ and $\theta = \frac{1}{2}$ can be found in [5] and [7] respectively, but for the reader's convenience, we show the details here:

Theorem 2.1 (see [5, 7]) *For the geometrically increasing step sizes $\{\Delta t_n\}$ given by (2.3) with $\tau > 1$, the matrix B can be diagonalized as $B = VDV^{-1}$, where $D = \text{diag}(\frac{1}{\theta\Delta_1}, \dots, \frac{1}{\theta\Delta_{N_t}})$. The eigenvector matrix V and its inverse are Toeplitz matrices of the form*

$$V = \begin{bmatrix} 1 & & & & \\ p_1 & 1 & & & \\ p_2 & p_1 & 1 & & \\ \vdots & \ddots & \ddots & \ddots & \\ p_{N_t-1} & \dots & p_2 & p_1 & 1 \end{bmatrix}, \quad V^{-1} = \begin{bmatrix} 1 & & & & \\ q_1 & 1 & & & \\ q_2 & q_1 & 1 & & \\ \vdots & \ddots & \ddots & \ddots & \\ q_{N_t-1} & \dots & q_2 & q_1 & 1 \end{bmatrix},$$

where

$$\begin{cases} p_n = \frac{1}{\prod_{j=1}^n (1 - \tau^j)}, & q_n = (-1)^n \tau^{\frac{n(n-1)}{2}} p_n, & \theta = 1, \\ p_n = \prod_{j=1}^n \frac{1 + \tau^j}{1 - \tau^j}, & q_n = q^{-n} \prod_{j=1}^n \frac{1 + \tau^{-j+2}}{1 - \tau^{-j}}, & \theta = \frac{1}{2}. \end{cases}$$

Now using the typical ParaDIAG factorization

$$B \otimes I_x + I_t \otimes A = (V \otimes I_x)(D \otimes I_x + I_t \otimes A)(V^{-1} \otimes I_x),$$

we can solve (2.6) by performing the three steps

$$\begin{aligned} \text{Step-(a)} \quad S_1 &= (V^{-1} \otimes I_x)\tilde{\mathbf{b}}, \\ \text{Step-(b)} \quad S_{2,n} &= \left(\frac{1}{\theta \Delta t_n} + A \right)^{-1} S_{1,n}, \quad n = 1, 2, \dots, N_t, \\ \text{Step-(c)} \quad \mathbf{u} &= (V \otimes I_x)S_2, \end{aligned} \quad (2.7)$$

where $S_1 = (S_{1,1}^\top, \dots, S_{1,N_t}^\top)^\top$ and $S_2 = (S_{2,1}^\top, \dots, S_{2,N_t}^\top)^\top$. Since V and V^{-1} are given in closed form, we only have to do matrix vector multiplications for Step-(a) and Step-(c), or one could use a fast Toeplitz solver based on Fourier techniques. For Step-(b), the N_t linear systems can be solved simultaneously in parallel. There is however an important issue with this direct time parallel solver ParaDIAG-I: if the time steps are very different, the truncation error of the time stepping scheme becomes worse, and if they are very close to each other, ParaDIAG-I suffers from roundoff error in the diagonalization used in Step-(a) and Step-(c). The best one can do is to balance the two errors, as a detailed analysis in [5, 7] shows, and this limits the applicability of ParaDIAG-I to shorter time intervals and few time steps: the roundoff error is proportional to the condition number of V , i.e.,

$$\text{roundoff error} \propto \text{Cond}_2(V).$$

If V is an eigenvector matrix of B , the *scaled* matrix $\tilde{V} = V\tilde{D}$ with any invertible diagonal matrix \tilde{D} is an eigenvector matrix of B as well. From [5, 7], the matrix $\tilde{D} = \text{diag}\left((1 + \sum_{j=1}^{N_t} |p_j|^2)^{-\frac{1}{2}}\right)$ is a good choice.

To illustrate the limitations of ParaDIAG-I, we provide the Matlab code `ParaDIAG_V1_for_ADE`, to test it for the advection-diffusion equation. For given T , N_t and τ the constraint $\sum_{n=1}^{N_t} \Delta t_n = T$ determines uniquely the value of the geometric time steps as

$$\Delta t_n = \frac{\tau^n}{\sum_{n=1}^{N_t} \tau^n} T. \quad (2.8)$$

For the space discretization, we fix $\Delta x = \frac{1}{64}$. To study the accuracy of ParaDIAG-I, we use a reference solution $\mathbf{u}_{\text{ode45}}$ obtained from the Matlab ODE solver `ode45` with a very small absolute and relative tolerance, `AbsTol`= 10^{-12} and `RelTol`= 10^{-12} , see Figure 2.1 for an illustration. The results of ParaDIAG-I compared to a sequential time integration are shown in Figure 2.2. We clearly see that using the geometric time steps (2.8) degrades the accuracy of the numerical solution, and when the time steps are too similar, the roundoff error problem sets in. This phenomenon was carefully studied in [5, 7], and the best possible geometrically stretched grid was determined, which leads to precise limits of time window length and number of time steps within which ParaDIAG-I can be reliably used.

2.2 ParaDIAG-II

Instead of using ParaDIAG as a direct solver with all different time steps to make the time stepping matrix diagonalizable, we can use it iteratively and solve a nearby problem in each iteration chosen such that the time stepping matrix of the nearby problem with uniform time step size can still be diagonalized. This idea leads to ParaDIAG algorithms in the ParaDIAG-II group. Among this group, we can use ParaDIAG within a stationary iteration or a Krylov subspace method. There are so far two very different ways to use ParaDIAG within a stationary iteration, proposed in [8] and [15]. The use of ParaDIAG within a Krylov subspace method can be found in [13, 18].

2.2.1 ParaDIAG-II – Waveform Relaxation (WR) Variant

The ParaDIAG algorithm introduced in [8] is based on the Waveform Relaxation iteration

$$\dot{U}^k(t) + AU^k(t) = 0, \quad U^k(0) = U_0 + \alpha(U^k(T) - U^{k-1}(T)), \quad t \in (0, T), \quad (2.9)$$

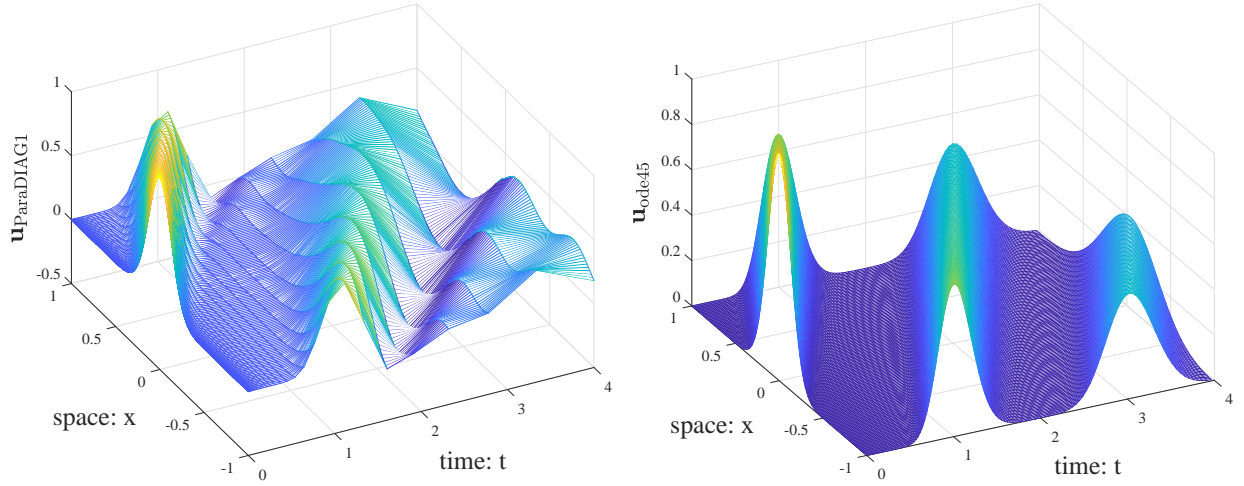


Figure 2.1: Left: numerical solution $\mathbf{u}_{\text{ParaDIAG-I}}$ obtained with $N_t = 64$ and $\tau = 1.2$. Right: reference solution $\mathbf{u}_{\text{ode45}}$. Here, $\nu = 10^{-2}$ and the Trapezoidal rule is used.

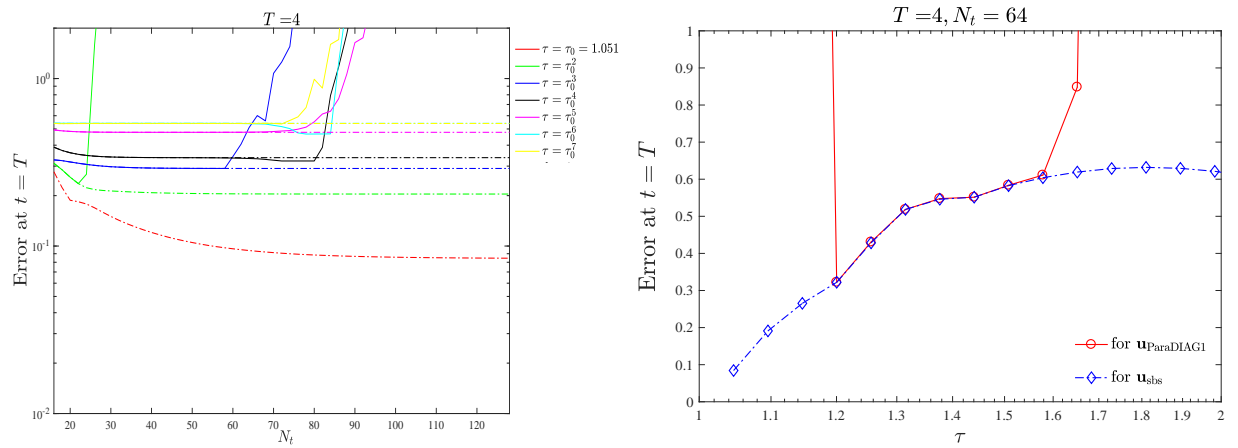


Figure 2.2: Left: using the geometric time steps (2.8) with 7 different τ the errors measured at the final time point $t = T$ for two numerical solutions: \mathbf{u}_{sbs} obtained step by step (dash-dot lines) and $\mathbf{u}_{\text{ParaDIAG-I}}$ obtained by (2.7) (solid lines). For $\mathbf{u}_{\text{ParaDIAG-I}}$ with $\tau = \tau_0 = 1.051$, the error is larger than 10^3 and thus the corresponding solid line is not shown. Right: for $N_t = 64$ the error for the two numerical solutions as τ varies. Here, $\nu = 10^{-2}$ and the Trapezoidal rule is used.

where $k \geq 1$ is the iteration index and $\alpha \in (0, 1]$ is a free parameter. Upon convergence, the tail term $\alpha(U^k(T) - U^{k-1}(T))$ is canceled and thus the converged solution is the solution of (2.2a). Applying the linear θ -method with a uniform step size Δt to (2.9) gives

$$\begin{cases} \frac{U_n^k - U_{n-1}^k}{\Delta t} + A(\theta U_n^k + (1-\theta)U_{n-1}^k) = 0, & n = 1, 2, \dots, N_t, \\ U_0^k = \alpha U_{N_t}^k - \alpha U_{N_t}^{k-1} + U_0, \end{cases} \quad (2.10)$$

where $N_t = T/\Delta t$. We rewrite (2.10) as an *all-at-once* system,

$$\left(C_1^{(\alpha)} \otimes I_x + C_2^{(\alpha)} \otimes A \right) \mathbf{u}^k = \mathbf{b}^{k-1}, \quad (2.11a)$$

where $\mathbf{u}^k = (U_1^k, \dots, U_{N_t}^k)^\top$, $C_1^{(\alpha)}, C_2^{(\alpha)} \in \mathbb{R}^{N_t \times N_t}$ and $\mathbf{b}^{k-1} \in \mathbb{R}^{N_t N_x}$ are given by

$$\begin{aligned} C_1^{(\alpha)} &= \frac{1}{\Delta t} \begin{bmatrix} 1 & & -\alpha \\ -1 & 1 & & \\ & \ddots & \ddots & \\ & & -1 & 1 \end{bmatrix}, \quad C_2^{(\alpha)} = \begin{bmatrix} \theta & & & (1-\theta)\alpha \\ 1-\theta & \theta & & \\ & \ddots & \ddots & \\ & & 1-\theta & \theta \end{bmatrix}, \\ \mathbf{b}^{k-1} &= \left((U_0 - \alpha U_{N_t}^{k-1}) \left(\frac{1}{\Delta t} I_x - (1-\theta)A \right), 0, \dots, 0 \right)^\top. \end{aligned} \quad (2.11b)$$

The matrices $C_{1,2}^{(\alpha)}$ are so-called α -circulant matrices and can be diagonalized as stated in Lemma 1, and we can again use the typical ParaDIAG factorization $C_1^{(\alpha)} \otimes I_x + C_2^{(\alpha)} \otimes A = (V \otimes I_x)(D_1 \otimes I_x + D_2 \otimes A)(V^{-1} \otimes I_x)$. Hence, similar to (2.7) we can solve (2.11a) performing the three steps

$$\begin{aligned} \text{Step-(a)} \quad & S_1 = (\mathbb{F} \otimes I_x)(\Gamma_\alpha \otimes I_x)\mathbf{b}^{k-1}, \\ \text{Step-(b)} \quad & S_{2,n} = (\lambda_{1,n} I_x + \lambda_{2,n} A)^{-1} S_{1,n}, \quad n = 1, 2, \dots, N_t, \\ \text{Step-(c)} \quad & \mathbf{u}^k = (\Gamma_\alpha^{-1} \otimes I_x)(\mathbb{F}^* \otimes I_x)S_2, \end{aligned} \quad (2.12)$$

where $D_j = \text{diag}(\lambda_{j,1}, \dots, \lambda_{j,N_t})$ and $j = 1, 2$. In (2.7), Step-(a) and Step-(c) can be computed efficiently via FFT and Step-(b) is again highly parallel. The eigenvector matrix V satisfies

$$\text{Cond}_2(V) = \text{Cond}_2(\Gamma_\alpha^{-1} \mathbb{F}^*) \leq \text{Cond}_2(\Gamma_\alpha^{-1}) \text{Cond}_2(\mathbb{F}^*) = \text{Cond}_2(\Gamma_\alpha^{-1}) \leq \frac{1}{\alpha}, \quad (2.13)$$

and thus the conditioning is depending on the choice of α . The convergence properties of this ParaDIAG-II algorithm are summarized in the following theorem.

Theorem 2.2 (see [8]) *For the linear system of ODEs $\dot{U}(t) + AU(t) = f$, suppose $\Re(\lambda(A)) \geq r \geq 0$ with $\lambda(A)$ being an arbitrary eigenvalue of A . Let \mathbf{u}^k be the k -th iterate of the ParaDIAG-II algorithm (2.10) with $\alpha \in (0, 1)$ and \mathbf{u} be the reference solution obtained by directly applying the same time-integrator to the system of ODEs. Then the linear convergence estimate $\|\mathbf{u}^k - \mathbf{u}\|_\infty \leq \rho^k \|\mathbf{u}^0 - \mathbf{u}\|_\infty$ holds, where*

$$\rho \leq \begin{cases} \frac{\alpha e^{-Tr}}{1-\alpha e^{-Tr}}, & \text{Backward-Euler,} \\ \frac{\alpha}{1-\alpha}, & \text{Trapezoidal rule.} \end{cases}$$

This shows that the ParaDIAG-II algorithm (2.10) converges with a rate independent of the spectrum of the matrix A and the step size of the time-discretization. The convergence factor ρ becomes smaller when α decreases, but the condition number of V (cf. (2.13)) implies that α can not be arbitrarily small (e.g., not of the size $\alpha = 10^{-13}$), because in this case the roundoff error will pollute the accuracy. The best parameter α_{opt} is again the value balancing the roundoff error and the discretization error, like for the direct solver ParaDIAG-I, see [8] for more discussions. In practice, $\alpha = 10^{-2}$ and $\alpha = 10^{-3}$ are good choices.

We provide a Matlab code, namely `ParaDIAG_V2_WR_for_ADE`, to test the ParaDIAG-II algorithm (2.10). In the code, we use the `fft` command to obtain $D_{1,2}$ by just using the first columns of $C_{1,2}^{(\alpha)}$, instead of the entire matrices. To implement Step-(a) in (2.12), we use the `fft` command as follows:

```
b=reshape(b,Nx,Nt); sol.stepA=fft(Gam.*(b.'));
```

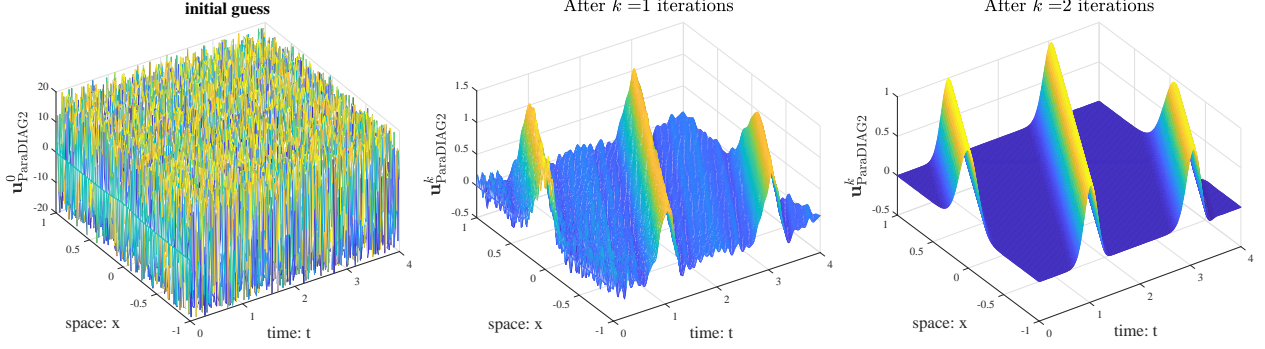


Figure 2.3: Initial guess and the first two iterates generated by the ParaDIAG-II algorithm (2.10) for $\nu = 10^{-4}$ and $\Delta x = \Delta t = \frac{1}{64}$.

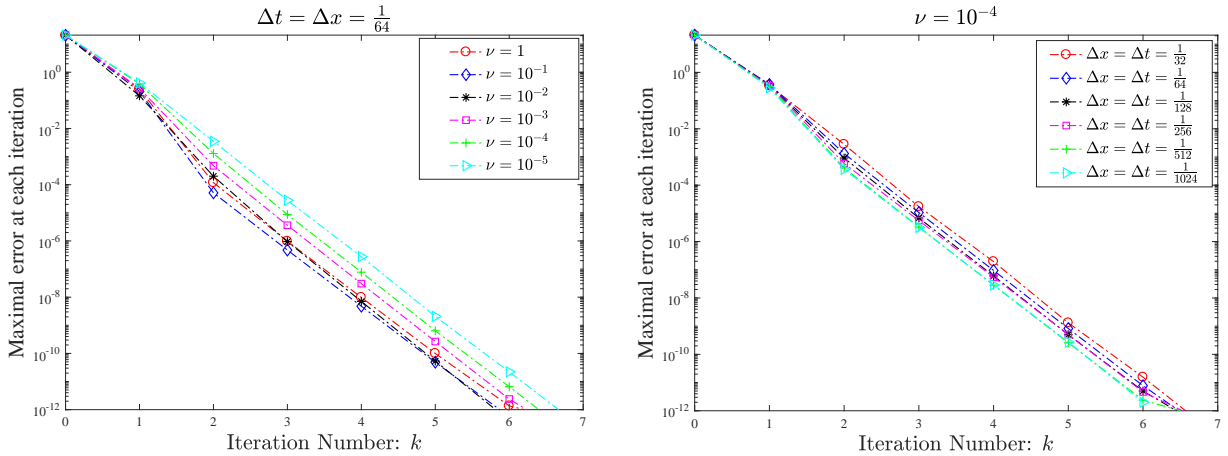


Figure 2.4: The convergence of the ParaDIAG-II algorithm (2.10) is robust with respect to ν , Δx and Δt . Here, $\alpha = 10^{-2}$ and the Trapezoidal rule is used as the time-integrator.

where b is the vector b^{k-1} . Similarly, to implement Step-(c) we use the inverse FFT command `ifft`,

$$Uk = (\text{invGam}.*\text{ifft}(\text{sol_stepB}.').');$$

Here, $\text{Gam} = (1, \alpha^{\frac{1}{N_t}}, \dots, \alpha^{\frac{N_t-1}{N_t}})$ and $\text{invGam} = (1, \alpha^{-\frac{1}{N_t}}, \dots, \alpha^{-\frac{1-N_t}{N_t}})$. With an initial guess chosen randomly as `random('unif', -20, 20, N_x, N_t)`, the first 2 iterates of this ParaDIAG-II algorithm are shown in Figure 2.3. The maximum error at each iteration is shown in Figure 2.4.

We next present some parallel speedup results for the ParaDIAG-II algorithm (2.10) based on Waveform Relaxation for a time-dependent advection-diffusion problem with periodic boundary conditions in 2D,

$$\begin{cases} \partial_t u(\mathbf{x}, t) - \nu \Delta u(\mathbf{x}, t) + \nabla u(\mathbf{x}, t) = 0, & \text{in } (0, T) \times \Omega, \\ u(\mathbf{x}, 0) = u_0(\mathbf{x}), & \text{in } \Omega, \end{cases} \quad (2.14)$$

where $\Omega = (0, 1) \times (0, 1)$ and $u_0(\mathbf{x}) = e^{-20[(x - \frac{1}{2})^2 + (y - \frac{1}{2})^2]}$. The results were obtained on the China Tianhe-1 supercomputer [19], which is a multi-array, configurable and cooperative parallel system with a theoretical peak performance of 1.372 petaflops, composed of high performance general-purpose microprocessors and a high-speed Infiniband network. We used the parallel Fortran library MUMPS (MULTifrontal Massively Parallel sparse direct Solver [1, 2]) version 4.10.0 to solve the linear systems in Step-(b) of (2.12). For Step-(a) and Step-(c), the `fft` and `ifft` commands are dissected into complex arithmetic operations. For the particular case when the source term is zero as shown in (2.11b), Step-(a) can be implemented in an economical way: only the first column of $(\mathbb{F} \otimes I_x)(\Gamma_\alpha \otimes I_x)$ is needed to compute S_1 .

Table 2.1: Iteration numbers of ParaDIAG-II (B-E), ParaDIAG-II (TR), Parareal and MGRiT in a strong scaling study, where $\Delta x = \Delta y = \Delta t = 1/128$ and $N_t = 512$. The symbol np indicates the number of processors and the coarsening factor is 8 in both parareal (two time levels) and MGRiT (three time levels).

np	$\nu = 10^0$				$\nu = 10^{-1}$				$\nu = 10^{-2}$				$\nu = 10^{-3}$				$\nu = 10^{-4}$				$\nu = 10^{-5}$			
	B-E	TR	PR	MG	B-E	TR	PR	MG	B-E	TR	PR	MG	B-E	TR	PR	MG	B-E	TR	PR	MG	B-E	TR	PR	MG
4	4	4	9	4	4	5	10	7	5	5	33	20	5	5	51	26	5	5	54	27	5	5	55	27
8	4	4	9	4	4	5	10	7	5	5	33	20	5	5	51	26	5	5	54	27	5	5	55	27
16	4	4	9	4	4	5	10	7	5	5	33	20	5	5	51	26	5	5	54	27	5	5	55	27
32	4	4	9	4	4	5	10	7	5	5	33	20	5	5	51	26	5	5	54	27	5	5	55	27
64	4	4	9	4	4	5	10	7	5	5	33	20	5	5	51	26	5	5	54	27	5	5	55	27
128	4	4	9	4	4	5	10	7	5	5	33	20	5	5	51	26	5	5	54	27	5	5	55	27

B-E: ParaDIAG-II (B-E), TR: ParaDIAG-II (TR), PR: parareal, MG: MGRiT

We provided the parallel codes in Fortran, which are zipped by a document labeled as 'Parallel Codes.zip'. For reader's convenience, the zip document contains a README file, in which we briefly introduce how to use these codes. Note that the modification of the Fortran library MUMPS (serving the purpose of serializing it in a distributed memory environment) is due to the fact that the relevant spatial solves are currently executed only in serial. In addition, a number of note statements are appended to Fortran's functions and subroutines. All the Fortran codes are compiled with mpich-3.1.3 using the `icc` compiler version 11.1.059 and `-O2` optimization level.

We denote by ParaDIAG-II (B-E) the algorithm (2.10) using Backward-Euler, and by ParaDIAG-II (TR) the one using the Trapezoidal rule, and set $\alpha = 0.02$. For comparison, we also apply the parareal algorithm and MGRiT to (2.14). The parareal algorithm is implemented using the two-level XBraid solver with F-relaxation, and MGRiT is the multilevel XBraid solver with FCF-relaxation (i.e., an initial F-relaxation followed by a C-relaxation and then a second F-relaxation). Furthermore, we skip the unnecessary work during the first XBraid down cycle for both the parareal and MGRiT algorithms, and fix the coarsening factor to 8. As shown in Table 2.1, ParaDIAG-II (B-E), ParaDIAG-II (TR), parareal and MGRiT converge robustly with respect to the number of processors. ParaDIAG-II (B-E) and ParaDIAG-II (TR) lead to parameter-robust convergence, while for parareal and MGRiT the required iteration counts increase dramatically as ν changes from 1 to 10^{-4} . The tolerance `tol` for all experiments here is set to $10^{-6}(< \min \frac{\{\Delta t^2, \Delta x^2\}}{10})$. In Figure 2.5 we compare the measured CPU times for these PinT algorithms. Clearly, ParaDIAG-II (B-E) and ParaDIAG-II (TR) are two optimally scaling PinT algorithms, while for MGRiT and parareal the scaling is a little bit worse (this is because of the sequential coarse-grid-correction as we will see in the next subsection). The corresponding data is given in Table 2.2. Regarding the parallel efficiency measured by

Table 2.2: Results for the strong scaling speedup of the four PinT algorithms measured by $T_{\text{cpu}}^{(4)}/T_{\text{cpu}}^{(n)}$, where $T_{\text{cpu}}^{(n)}$ is the wall-clock time using n processors.

ν	parareal				MGRiT				ParaDIAG-II (B-E)				ParaDIAG-II (TR)			
	16	32	64	128	16	32	64	128	16	32	64	128	16	32	64	128
10^0	1.94	2.28	2.49	2.69	2.93	4.33	5.28	7.00	3.96	7.54	15.20	29.03	3.90	7.73	15.13	28.47
10^{-1}	1.95	2.30	2.53	2.80	3.03	4.72	5.57	7.41	4.03	7.86	15.53	30.93	3.89	7.75	15.03	29.00
10^{-2}	1.96	2.32	2.56	2.83	2.99	4.58	5.62	7.35	3.90	7.76	15.23	29.00	3.91	7.77	15.20	28.84
10^{-3}	1.97	2.33	2.57	2.85	2.99	4.58	5.61	7.37	3.87	7.33	15.23	29.85	3.87	7.72	15.14	28.63
10^{-4}	1.95	2.31	2.55	2.82	2.95	4.55	5.61	7.33	3.89	7.74	15.17	29.57	3.91	7.72	15.29	29.95
10^{-5}	1.94	2.30	2.54	2.81	2.99	4.46	5.64	7.35	3.56	7.75	15.15	28.37	3.89	7.72	15.15	29.26

$T_{\text{cpu}}^{(4)}/(32 \times T_{\text{cpu}}^{(128)})$ [14] ($T_{\text{cpu}}^{(n)}$ is the wall-clock time using n processors), the average parallel efficiency for ParaDIAG-II (B-E) is 92.06%, for ParaDIAG-II (TR) it is 90.70%, while it is only 22.82% for MGRiT and 8.75% for parareal.

2.2.2 ParaDIAG-II – Parareal Variant

The second way to use ParaDIAG within a stationary iteration is based on formulating the coarse-grid-correction (CGC) procedure of the parareal algorithm [9,10] as an all-at-once system and applying ParaDIAG

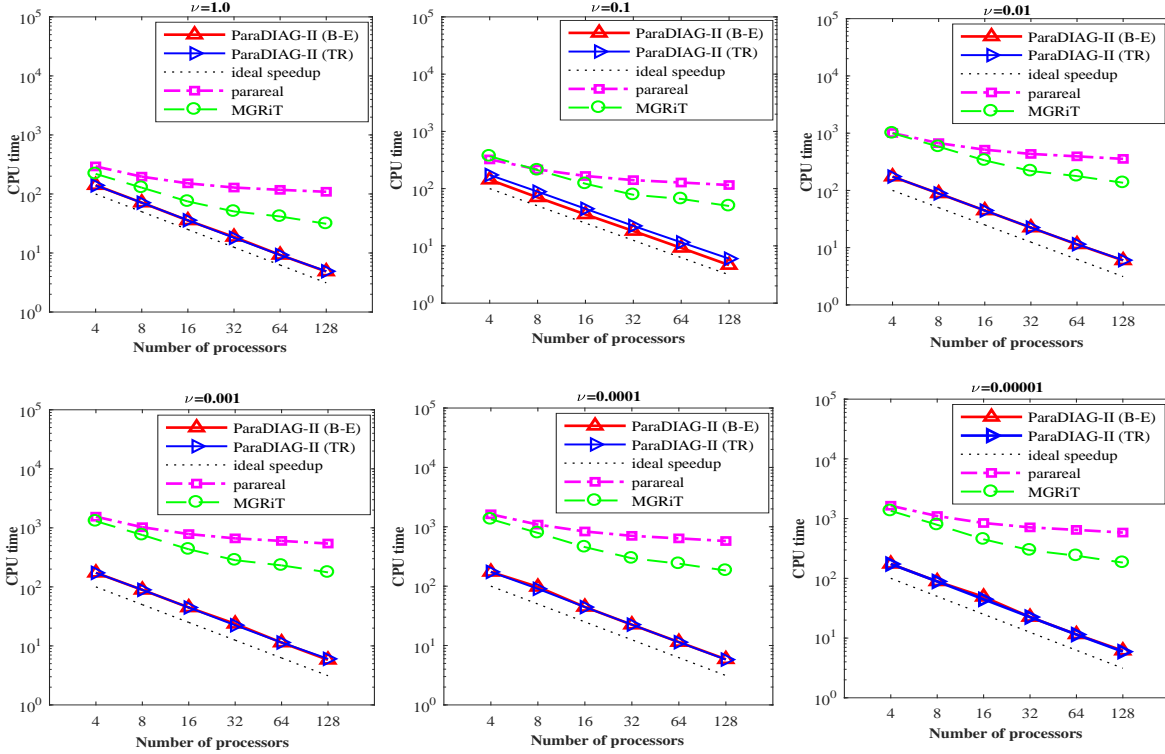


Figure 2.5: Comparison of the overall time-to-solution in a strong scaling study, where $\Delta x = \Delta y = \Delta t = 1/128$ and $N_t = 512$. The coarsening factor is $cf=8$ for both parareal and MGRIT.

to it. The parareal algorithm is an iterative PinT algorithm, based on the updating formula

$$U_{n+1}^k = \mathcal{F}^J(\Delta t, U_n^{k-1}) + \mathcal{G}(\Delta t, U_n^k) - \mathcal{G}(\Delta t, U_n^{k-1}), \quad n = 0, 1, \dots, N_t - 1, \quad (2.15)$$

where \mathcal{G} and \mathcal{F} are called coarse and fine propagator, specified by two time-integrators. The quantity $\mathcal{F}^J(\Delta t, U_n^{k-1})$ denotes a value calculated by applying successively J steps of the fine propagator \mathcal{F} to the differential equations with initial value U_n^{k-1} and the fine step size Δt . The integer $J = \frac{\Delta T}{\Delta t} \geq 2$ is called the *coarsening ratio*. Let

$$b_{n+1}^{k-1} := \mathcal{F}^J(\Delta t, U_n^{k-1}) - \mathcal{G}(\Delta t, U_n^{k-1}).$$

Then, the parareal algorithm is $U_{n+1}^k = \mathcal{G}(\Delta t, U_n^k) + b_{n+1}^{k-1}$. This is the so called CGC, which is a sequential procedure and is often the bottleneck of the parallel efficiency. In [15], the author proposed an idea to parallelize the CGC: supposing we have to solve an initial-value problem

$$\dot{U}(t) + f(U(t)) = 0, \quad U(0) = U_0,$$

we apply \mathcal{G} to a slightly *wrong* problem, namely

$$\dot{U}(t) + f(U(t)) = 0, \quad U(0) = \alpha U(T),$$

where $\alpha \in (0, 1)$ is a free parameter. We use the linear case $f(U) = AU$ to illustrate the details of ParaDIAG-II based on the parareal algorithm (for the nonlinear case, see [15]). We also use for simplicity Backward-Euler for \mathcal{G} . Let $\tilde{U}_{n+1} := \mathcal{F}^J(\Delta t, U_n^{k-1})$. The quantity $\mathcal{G}(\Delta t, U_n^{k-1})$ computed from the previous iteration is

$$\mathcal{G}(\Delta t, U_n^{k-1}) = \begin{cases} \alpha(I_x + \Delta T A)^{-1} U_{N_t}^{k-1}, & n = 0, \\ (I_x + \Delta T A)^{-1} U_n^{k-1}, & n = 1, 2, \dots, N_t - 1. \end{cases}$$

Note that all the N_t quantities $\{\tilde{U}_n\}_{n=1}^{N_t}$ and $\{\mathcal{G}(\Delta t, U_n^{k-1})\}_{n=0}^{N_t-1}$ can be computed simultaneously in parallel. Hence, $b_{n+1}^{k-1} = \tilde{U}_{n+1} - \mathcal{G}(\Delta t, U_n^{k-1})$. The parareal algorithm (2.15) can be rewritten as

$$(I_x + \Delta T A)U_{n+1}^k = U_n^k + (I_x + \Delta T A)b_{n+1}^{k-1} \implies \frac{U_{n+1}^k - U_n^k}{\Delta T} + AU_{n+1}^k = (\Delta T^{-1}I_x + A)b_{n+1}^{k-1},$$

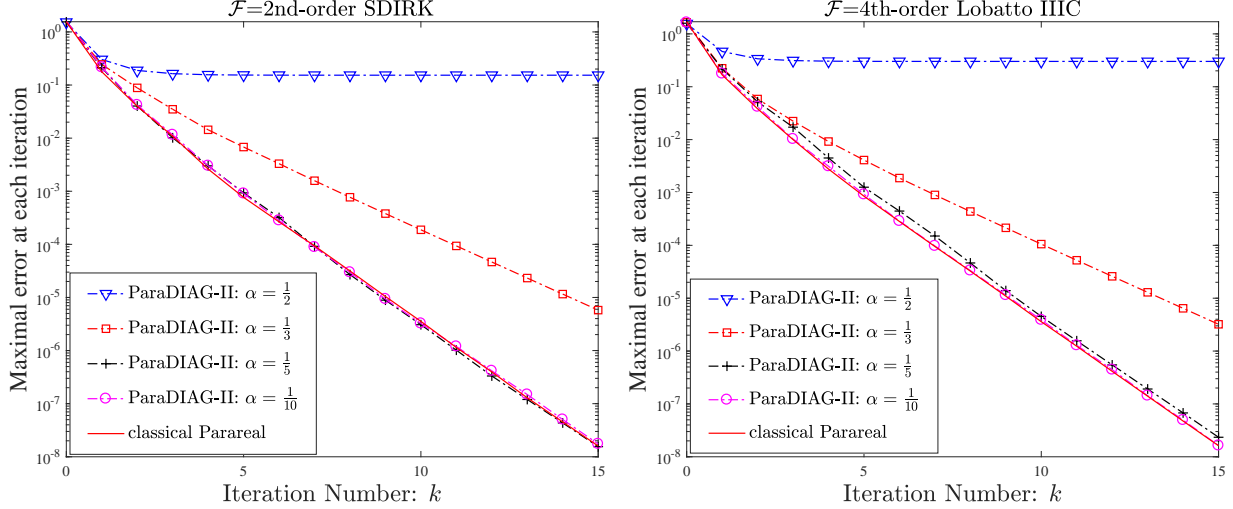


Figure 2.6: For $\nu = 10^{-1}$, $T = 4$, $\Delta x = \frac{1}{64}$, $\Delta T = \frac{1}{16}$ and $J = 32$, the measured error of ParaDIAG-II parareal compared to classical parareal.

where $U_0^k = \alpha U_{N_t}^k$, which can be represented as

$$\underbrace{\frac{1}{\Delta T} \begin{bmatrix} 1 & & & -\alpha \\ -1 & 1 & & \\ & \ddots & \ddots & \\ & & -1 & 1 \end{bmatrix} \otimes I_x + \begin{bmatrix} A & & & \\ & A & & \\ & & \ddots & \\ & & & A \end{bmatrix}}_{=C_1^{(\alpha)} \otimes I_x} \underbrace{\begin{bmatrix} U_1^k \\ U_2^k \\ \vdots \\ U_{N_t}^k \end{bmatrix}}_{=\mathbf{u}^k} = \underbrace{\begin{bmatrix} (\Delta T^{-1} I_x + A) \tilde{U}_1^k - \alpha \Delta T^{-1} U_{N_t}^{k-1} \\ (\Delta T^{-1} I_x + A) \tilde{U}_2^k - \Delta T^{-1} U_1^{k-1} \\ \vdots \\ (\Delta T^{-1} I_x + A) \tilde{U}_{N_t}^k - \Delta T^{-1} U_{N_t-1}^{k-1} \end{bmatrix}}_{=\mathbf{b}^k}.$$

This problem is now precisely of the form (2.10) for $\theta = 1$, i.e. the Backward-Euler method, and the solution \mathbf{u}^k can be obtained using ParaDIAG-II (cf. 2.12). The convergence rate of this ParaDIAG-II parareal variant is summarized in the following theorem.

Theorem 2.3 (see [15]) *Let $\rho_{\text{SinT-CGC}}$ be the convergence factor of the parareal algorithm with sequential-in-time CGC (i.e., the classical parareal algorithm) and $\rho_{\text{PinT-CGC}}$ be the convergence factor with parallel-in-time CGC. Then, there exists some threshold α^* of the parameter α , such that*

$$\rho_{\text{PinT-CGC}} = \rho_{\text{SinT-CGC}}, \text{ if } 0 < \alpha \leq \alpha^*.$$

In particular, for linear systems of ODEs $\dot{U}(t) + AU(t) = f$ with $\sigma(A) \subset [0, \infty)$, i.e., all the eigenvalues of A are non-negative real numbers, if we choose for \mathcal{G} the Backward-Euler method and for \mathcal{F} an L-stable time-integrator (e.g., the Radau IIA methods and the Lobatto IIIC methods), it holds that $\alpha^ \approx 0.3$.*

This implies that if α does not exceed the threshold α^* , the ParaDIAG-II parareal algorithm has the same convergence rate as the classical parareal algorithm.

We provided a Matlab code, namely `ParaDIAG_V2_Parareal_for_ADE`, to test the convergence of the ParaDIAG-II parareal algorithm. The code includes a function `choose_F`, which provides 4 choices for the \mathcal{F} -propagator: the Backward-Euler method, the 2nd-order SDIRK (Singly Diagonally Implicit Runge-Kutta) method, the 3rd-order Radau IIA method and the 4th-order Lobatto IIIC method. The interested reader can add more choices for \mathcal{F} in this function. Moreover, we deal with a single step of the \mathcal{F} -propagator by a function `Pro_F`. The diagonalization procedure is still implemented via the `fft` and `ifft` commands. Starting from a random initial guess, the error at each iteration of the new ParaDIAG-II parareal algorithm is shown in Figure 2.6. The ParaDIAG-II parareal algorithm converges as fast as the classical parareal algorithm when $\alpha \leq \frac{1}{5}$. We mention that there is also a MGRiT variant of ParaDIAG-II [17], which uses different *head-tail* coupled condition together with the diagonalization technique for parallel CGC procedure.

3 ParaDIAG-II – Krylov Variant (for wave equations)

It is a longstanding challenging task to design efficient PinT algorithms for wave propagation problems. The ParaDIAG-II WR algorithm [8] can handle such problems, with rapid, robust and analyzable convergence rate. (Both the Parareal variant [15] and MGRIIT variant [17] of ParaDIAG-II can NOT handle wave equations.) The WR variant of ParaDIAG-II is an algorithm used within a stationary iteration. Here, we present a ParaDIAG-II variant to be used within a Krylov subspace method, and which is also applicable to wave equations. A further advantage of the new variant is that it can also efficiently handle optimal control problems of wave equations as described in Section 4, while currently some basic tools are lacking (at least at the moment) to handle such optimal control problems via ParaDIAG-II WR.

The idea below was first introduced by McDonald, Pestana and Wathen in [13] for parabolic problems, but here we show that a key modification makes it a good solver also for wave propagation problems. We consider the linear wave equation

$$\begin{cases} u_{tt} - \Delta u = f, & \text{in } \Omega \times (0, T), \\ u = 0, & \text{on } \partial\Omega \times (0, T), \\ u(\cdot, 0) = u_0, \quad u_t(\cdot, 0) = u_1, & \text{in } \Omega, \end{cases} \quad (3.1)$$

where $\Omega \subset \mathbb{R}^d$ with $d \geq 1$ is the space domain, u_0 and u_1 are given compatible initial conditions and f is a given source term. We discretize (3.1) in time by the implicit leap-frog finite difference scheme [11] (but other schemes can be adopted as well), which was shown to be unconditionally stable without imposing the restrictive Courant–Friedrichs–Lewy (CFL) condition on spatial and temporal mesh sizes. Similar to the advection-diffusion equation, we can represent the space and time discretizations by an all-at-once system,

$$\mathbf{A}\mathbf{u} := (B_1 \otimes I_x + B_2 \otimes A) \mathbf{u} = \mathbf{b}, \quad (3.2a)$$

where $A \in \mathbb{R}^{N_x \times N_x}$ is the discrete matrix of the negative Laplacian $-\Delta$, and

$$B_1 = \frac{1}{\Delta t^2} \begin{bmatrix} 1 & & & & \\ -2 & 1 & & & \\ 1 & -2 & 1 & & \\ \ddots & \ddots & \ddots & \ddots & \\ & 1 & -2 & 1 \end{bmatrix}, \quad B_2 = \frac{1}{2} \begin{bmatrix} 1 & & & & \\ 0 & 1 & & & \\ 1 & 0 & 1 & & \\ \ddots & \ddots & \ddots & \ddots & \\ 1 & 0 & 1 \end{bmatrix} \in \mathbb{R}^{N_t \times N_t}. \quad (3.2b)$$

The idea in [13] for solving (3.2a) is to construct a circulant block preconditioner $\mathbf{P} = C_1 \otimes I_x + C_2 \otimes A$, obtained by replacing the two Toeplitz matrices B_1 and B_2 in (3.2b) by the two Strang circulant matrices

$$C_1 = \frac{1}{\Delta t^2} \begin{bmatrix} 1 & & 1 & -2 \\ -2 & 1 & & 1 \\ 1 & -2 & 1 & \\ \ddots & \ddots & \ddots & \\ 1 & -2 & 1 \end{bmatrix}, \quad C_2 = \frac{1}{2} \begin{bmatrix} 1 & & 1 & \\ 0 & 1 & & \\ 1 & 0 & 1 & \\ \ddots & \ddots & \ddots & \ddots \\ 1 & 0 & 1 \end{bmatrix}. \quad (3.3)$$

Unfortunately, as we will see later in Table 3.1, this preconditioner does not achieve satisfactory convergence rates for wave equations of the form (3.1), in contrast to parabolic equations for which it was designed in [13].

The new idea of ParaDIAG-II is to use a generalized preconditioner $\mathbf{P}_\alpha = \frac{1}{\Delta t^2} C_1^{(\alpha)} \otimes I_x + C_2^{(\alpha)} \otimes A$ by replacing B_1 and B_2 by α -circulant matrices (with $\alpha \in (0, 1]$ again a free parameter), where

$$C_1^{(\alpha)} = \frac{1}{\Delta t^2} \begin{bmatrix} 1 & & \alpha & -2\alpha \\ -2 & 1 & & \alpha \\ 1 & -2 & 1 & \\ \ddots & \ddots & \ddots & \\ 1 & -2 & 1 \end{bmatrix}, \quad C_2^{(\alpha)} = \frac{1}{2} \begin{bmatrix} 1 & & \alpha & \\ 0 & 1 & & \alpha \\ 1 & 0 & 1 & \\ \ddots & \ddots & \ddots & \ddots \\ 1 & 0 & 1 \end{bmatrix}. \quad (3.4)$$

According to Lemma 1, these two α -circulant matrices $C_1^{(\alpha)}$ and $C_2^{(\alpha)}$ can be simultaneously diagonalized as $C_{1,2}^{(\alpha)} = V D_{1,2} V^{-1}$ and thus for an input vector r the inversion computation of $\mathbf{P}_\alpha^{-1}r$ can be performed by ParaDIAG (cf. (1.5)): let $D = I_x + \frac{\Delta t^2}{2} A$ and $D = Q \text{diag}(\lambda_1, \dots, \lambda_{N_x}) Q^T$ be the spectral decomposition of D with an orthogonal matrix Q and a real diagonal matrix $\text{diag}(\lambda_1, \dots, \lambda_{N_x})$ including all the sorted (increasing) eigenvalues. We have the following result for the spectrum of the preconditioned matrix $\mathbf{P}_\alpha^{-1}M$:

Table 3.1: ParaDIAG-II – GMRES for two values of the parameter α

(N_x, N_t)	$\alpha = 1$				$\alpha = 0.1$			
	Error	Order	Iter	CPU	Error	Order	Iter	CPU
(32,32,33)	7.17E-03	1.9	3	0.07	7.17E-03	1.9	3	0.04
(64,64,65)	1.86E-03	1.9	7	0.57	1.86E-03	1.9	3	0.31
(128,128,129)	4.74E-04	2.0	37	24.25	4.74E-04	2.0	3	2.17
(256,256,257)			>50		1.20E-04	2.0	3	21.02

Theorem 3.1 (see [18]) *The eigenvalues of the matrix $\mathbf{P}_\alpha^{-1} \mathbf{M}$ are explicitly given by*

$$\sigma(\mathbf{P}_\alpha^{-1} \mathbf{M}) = \underbrace{\{1, 1, \dots, 1\}}_{(N_t-2)N_x} \cup \left\{ \frac{1}{1 - \alpha e^{\pm i N_t \theta_j}} \right\}_{j=1}^{N_x},$$

where $\theta_j := \arctan(\sqrt{\lambda_j^2 - 1}) \in (0, \pi/2)$. Moreover, we further have the estimates:

1. If $\alpha \in (0, 1)$, then

$$\sigma(\mathbf{P}_\alpha^{-1} \mathbf{M}) \subset \mathbb{A}_\alpha := \left\{ z \in \mathbb{C} : \frac{\alpha}{1 + \alpha} \leq |z| \leq \frac{\alpha}{1 - \alpha} \right\}.$$

2. If $\alpha = 1$, then

$$\sigma(\mathbf{P}_\alpha^{-1} \mathbf{M}) = \{1\} \cup \left\{ \frac{1}{2} \pm \frac{1}{2} i \cot\left(\frac{N_t \theta_j}{2}\right) \right\}_{j=1}^{N_x}.$$

We provide a Matlab code `ParaDIAG_V2_GMRES_LinearWave_2D` to solve a 2D wave equation example with

$$T = 2, u_0(x, y) = \sin(\pi x) \sin(\pi y), \quad u_1(x, y) = \sin(\pi x) \sin(\pi y), \quad f = (1 + 2\pi^2) \sin(\pi x) \sin(\pi y) e^t,$$

where the exact solution is $u(x, y, t) = \sin(\pi x) \sin(\pi y) e^t$. Here we choose a zero initial guess and a stopping tolerance $\text{tol} = 10^{-10}$ based on the reduction in relative residual norms. The complex-shifted systems in Step-(b) are solved by MATLAB's sparse direct solver. We will measure the discrete $L^\infty((0, T); L^2(\Omega))$ error norms of the numerical approximation, and then estimate the experimental order of accuracy by calculating the logarithmic ratio of the approximation errors between two successively refined meshes, i.e.,

$$\text{Order} = \log_2 \left(\frac{\text{Error}(h, \tau)}{\text{Error}(2h, 2\tau)} \right),$$

which should be close to 2 for second-order accuracy. As we can see from Table 3.1, the iteration numbers for the preconditioner with the original choice of $\alpha = 1$ grow dramatically when the mesh is refined. This is much better with the smaller choice $\alpha = 0.1$ in the new ParaDIAG-II algorithm, where we observe only 3 iterations. The CPU times also show the expected quasilinear time complexity of ParaDIAG-II.

4 ParaDIAG-II – Krylov Variant (for optimal control of the wave equation)

The Krylov variant of ParaDIAG-II can also be used to handle optimal control problems of the wave equation [18], by applying ParaDIAG as a preconditioner for the discrete saddle-point system within the framework of Krylov subspace methods. Let $\Omega \in \mathbb{R}^d$ with $d \geq 1$ be a bounded and open domain with Lipschitz boundary, and $[0, T]$ be the time window of interest with $T > 0$. We consider a distributed optimal control problem of minimizing a tracking-type quadratic cost functional,

$$\min_{u, \tilde{u}} \mathcal{L}(u, u) := \frac{1}{2} \|u - g\|_{L^2(\Omega \times (0, T))}^2 + \frac{\gamma}{2} \|\tilde{u}\|_{L^2(\Omega \times (0, T))}^2, \quad (4.1a)$$

subject to a linear wave equation with initial- and boundary conditions

$$\begin{cases} u_{tt} - \Delta y = f + \tilde{u}, & \text{in } \Omega \times (0, T), \\ u = 0, & \text{on } \partial\Omega \times (0, T), \\ u(\cdot, 0) = u_0, \quad u_t(\cdot, 0) = u_1, & \text{in } \Omega, \end{cases} \quad (4.1b)$$

where $\tilde{u} \in L^2$ is the distributed control, $g \in L^2$ is the desired tracking trajectory or observation data and $\gamma > 0$ is the cost weight or regularization parameter. The first-order optimality system of (4.1a)-(4.1b) is

$$\begin{cases} u_{tt} - \Delta u - \frac{1}{\gamma}p = f, & \text{in } \Omega \times (0, T), \quad y = 0, \text{ on } \partial\Omega \times (0, T), \\ u(\cdot, 0) = u_0, \quad u_t(\cdot, 0) = u_1, & \text{in } \Omega, \\ p_{tt} - \Delta p + u = g, & \text{in } \Omega \times (0, T), \quad p = 0, \text{ on } \partial\Omega \times (0, T), \\ p(\cdot, T) = 0, \quad p_t(\cdot, T) = 0, & \text{in } \Omega, \end{cases} \quad (4.2)$$

where we have eliminated the control variable \tilde{u} from the optimality condition $\gamma\tilde{u} - p = 0$ in (4.2), leading to a reduced optimality system regarding only u and p .

By using the implicit leap-frog finite difference scheme [11] we get the discrete saddle-point system

$$\widehat{\mathbf{A}} \begin{bmatrix} \mathbf{u} \\ \mathbf{p} \end{bmatrix} := \left(\begin{bmatrix} B_1 & -\frac{\Delta t^2 \hat{I}_t}{\gamma} \\ \Delta t^2 \check{I}_t & B_1^\top \end{bmatrix} \otimes I_x + \frac{\Delta t^2}{2} \begin{bmatrix} B_2 & \\ & B_2^\top \end{bmatrix} \otimes A \right) \begin{bmatrix} \mathbf{u} \\ \mathbf{p} \end{bmatrix} = \begin{bmatrix} \mathbf{f} \\ \mathbf{g} \end{bmatrix},$$

where $\hat{I}_t = \text{diag}(\frac{1}{2}, 1, \dots, 1)$, $\check{I}_t = \text{diag}(1, \dots, 1, \frac{1}{2}) \in \mathbb{R}^{N_t \times N_t}$, $A \in \mathbb{R}^{N_x \times N_x}$ is the discrete matrix of the negative Laplacian $-\Delta$ and $B_{1,2}$ are the Toeplitz matrices given by (3.2b). The idea in [18] for applying the ParaDIAG algorithm lies in three steps. First, we need to balance the effect of the regularization parameter γ via a similarity transform

$$\underbrace{\left(\begin{bmatrix} \gamma^{\frac{1}{2}} I_t & \\ & I_t \end{bmatrix} \otimes I_x \right) \widehat{\mathbf{A}} \left(\begin{bmatrix} \gamma^{-\frac{1}{2}} I_t & \\ & I_t \end{bmatrix} \otimes I_x \right)}_{:= \mathbf{A}} \begin{bmatrix} \gamma^{\frac{1}{2}} \mathbf{u} \\ \mathbf{p} \end{bmatrix} = \begin{bmatrix} \gamma^{\frac{1}{2}} \mathbf{f} \\ \mathbf{g} \end{bmatrix},$$

where $\mathbf{A} = \begin{bmatrix} B_1 & -\frac{\Delta t^2 \hat{I}_t}{\sqrt{\gamma}} \\ \frac{\Delta t^2 \check{I}_t}{\sqrt{\gamma}} & B_1^\top \end{bmatrix} \otimes I_x + \frac{\Delta t^2}{2} \begin{bmatrix} B_2 & \\ & B_2^\top \end{bmatrix} \otimes A$. Second, based on the Toeplitz structure we propose the following block circulant preconditioner

$$\mathbf{P} := \begin{bmatrix} C_1 & -\frac{\Delta t^2 I_t}{\sqrt{\gamma}} \\ \frac{\Delta t^2 I_t}{\sqrt{\gamma}} & C_1^\top \end{bmatrix} \otimes I_x + \frac{\Delta t^2}{2} \begin{bmatrix} C_2 & \\ & C_2^\top \end{bmatrix} \otimes A,$$

where C_1 and C_2 are given by (3.3). Note that the diagonal matrices \hat{I}_t and \check{I}_t are replaced by the identity matrix $I_t \in \mathbb{R}^{N_t \times N_t}$. The last step is to rewrite \mathbf{P} as

$$\mathbf{P} = \underbrace{\left(\begin{bmatrix} C_1 C_2^{-1} & -\frac{\Delta t^2 (C_2^{-1})^\top}{\sqrt{\gamma}} \\ \frac{\Delta t^2 C_2^{-1}}{\sqrt{\gamma}} & C_1^\top (C_2^{-1})^\top \end{bmatrix} \otimes I_x + \frac{\Delta t^2}{2} \begin{bmatrix} I_t & \\ & I_t \end{bmatrix} \otimes A \right)}_{=: \tilde{\mathbf{P}}} \left(\begin{bmatrix} C_2 & \\ & C_2^\top \end{bmatrix} \otimes I_x \right). \quad (4.3)$$

Now, for any input vector r , we can compute $s = \mathbf{P}^{-1}r$ via

$$\tilde{s} := \begin{bmatrix} \tilde{s}_1 \\ \tilde{s}_2 \end{bmatrix} = \tilde{\mathbf{P}}^{-1}r, \quad s = \begin{bmatrix} (C_2^{-1} \otimes I_x) \tilde{s}_1 \\ ((C_2^{-1})^\top \otimes I_x) \tilde{s}_2 \end{bmatrix}.$$

Once \tilde{s} is calculated, we can compute s with high efficiency by the fast Fourier transform (FFT). Hence, the major computation is to compute $\tilde{s} = \tilde{\mathbf{P}}^{-1}r$. We now derive a special diagonalization of the matrix $\tilde{\mathbf{P}}$ in (4.3). The reason why we split \mathbf{P}^{-1} into two steps is that we do not have a spectral decomposition of \mathbf{P} with a closed formula. For $\tilde{\mathbf{P}}$, we have the following spectral decomposition.

Table 4.1: Number of GMRES iterations and CPU times using the ParaDIAG-II preconditioner \mathbf{P} .

$\text{tol} = 10^{-7}$	$\gamma = 10^{-2}$		$\gamma = 10^{-4}$		$\gamma = 10^{-6}$		$\gamma = 10^{-8}$		$\gamma = 10^{-10}$	
(N_x, N_x, N_t)	It	CPU	It	CPU	It	CPU	It	CPU	It	CPU
(16,16,17)	5	0.0	5	0.0	5	0.0	4	0.0	4	0.0
(32,32,33)	5	0.1	5	0.2	5	0.1	5	0.1	4	0.1
(64,64,65)	5	0.7	5	1.1	5	0.8	5	0.8	4	0.6
(128,128,129)	11	13.9	5	7.2	5	6.7	5	6.4	5	6.7
(256,256,257)	17	226.6	5	59.6	5	60.3	5	61.0	5	60.7

Theorem 4.1 (see [16]) *Let D_1 and D_2 be the diagonal matrices consisting of the circulant matrices C_1 and C_2 and $\mathbb{F} \in \mathbb{C}^{N_t \times N_t}$ be the discrete Fourier matrix. The matrix $\tilde{\mathbf{P}}$ in (4.3) can be factorized as*

$$\tilde{\mathbf{P}} = (V \otimes I_x) \left(\begin{bmatrix} \Sigma_1 & \\ & \Sigma_2 \end{bmatrix} \otimes I_x + \frac{\Delta t^2}{2} \begin{bmatrix} I_t & \\ & I_t \end{bmatrix} \otimes A \right) (V^{-1} \otimes I_x). \quad (4.4a)$$

where

$$V = \begin{bmatrix} \mathbb{F}^* & \\ & \mathbb{F}^* \end{bmatrix} \begin{bmatrix} I_t & -i\sqrt{D_2^* D_2^{-1}} \\ i\sqrt{D_2^* D_2^{-1}} & I_t \end{bmatrix}, \quad V^{-1} = \frac{1}{2} V^*, \quad (4.4b)$$

$$\Sigma_1 = D_1 D_2^{-1} + i \frac{\Delta t^2}{\sqrt{\gamma}} |D_2^{-1}|, \quad \Sigma_2 = D_1 D_2^{-1} - i \frac{\Delta t^2}{\sqrt{\gamma}} |D_2^{-1}|.$$

Let \tilde{D} be an invertible diagonal matrix. Then, it is clear that the factorization (4.4a) still holds if we replace V by $V\tilde{D}$. Hence the eigenvector matrix for the block diagonalization of $\tilde{\mathbf{P}}$ is not unique. A nice property of the factorization given by (4.4a)-(4.4b) is that the matrix V is *optimal* in the sense that $\text{Cond}_2(V) = 1$. According to (4.4b), for any input vector \mathbf{r} we can compute $\tilde{\mathbf{P}}^{-1}\mathbf{r}$ by the diagonalization technique described in (1.5). It was shown in [16] that the eigenvalues of the non-symmetric preconditioned matrix $\mathbf{P}^{-1}\mathbf{A}$ are highly clustered (the similarity transform from $\hat{\mathbf{A}}$ to \mathbf{A} is important for this).

We provide a Matlab code `ParaDIAG_V2_GMRES_LinearWaveOPT_2D` for the 2D wave equation optimal control problem posed on $\Omega \times (0, T) = (0, 1)^2 \times (0, 2)$, with the data

$$u_0(x, y) = \sin(\pi x) \sin(\pi y), \quad u_1(x, y) = \sin(\pi x) \sin(\pi y),$$

$$f(x, y, t) = (1 + 2\pi^2)e^t \sin(\pi x) \sin(\pi y) - \frac{1}{\gamma}(t - T)^2 \sin(\pi x) \sin(\pi y),$$

$$g(x, y, t) = (e^t + 2 + 2\pi^2(t - T)^2) \sin(\pi x) \sin(\pi y).$$

The exact solution of the optimal control problem is

$$u(x, y, t) = e^t \sin(\pi x) \sin(\pi y) \quad \text{and} \quad p(x, y, t) = (t - T)^2 \sin(\pi x) \sin(\pi y).$$

As shown in Table 4.1, GMRES preconditioned with the ParaDIAG-II preconditioner \mathbf{P} converges very fast and is robust with respect to the possibly very small regularization parameter γ .

References

- [1] P. R. Amestoy, A. Buttari, J.-Y. L'Excellent, and T. Mary. *Performance and scalability of the block low-rank multifrontal factorization on multicore architectures*. ACM Trans. Math. Softw., Vol 45, pp 2:1-2:26, 2019.
- [2] P. R. Amestoy, I. S. Duff, J. Koster, and J.-Y. L'Excellent. *A fully asynchronous multifrontal solver using distributed dynamic scheduling*. SIAM J. Matrix Anal. Appl., Vol 23, pp 15-41, 2001.
- [3] D. A. Bini, G. Latouche, and B. Meini. *Numerical Methods for Structured Markov Chains*, Oxford University Press, 2005.

- [4] M. J. Gander. *Analysis of the Parareal Algorithm Applied to Hyperbolic Problems Using Characteristics*, Bol. Soc. Esp. Mat. Apl., Vol. 42, pp. 21-35, 2008.
- [5] M. J. Gander, L. Halpern, J. Rannou, and J. Ryan. *A direct solver for time parallelization*. in: Domain Decomposition Methods in Science and Engineering XXII. Springer, pp. 491-499, 2016.
- [6] M. J. Gander and L. Halpern. *Time parallelization for nonlinear problems based on diagonalization*, in: Domain Decomposition Methods in Science and Engineering XXIII, Springer, pp. 163-170, 2017.
- [7] M. J. Gander, L. Halpern, J. Rannou, and J. Ryan. *A direct time parallel solver by diagonalization for the wave equation*. SIAM J. Sci. Comput., Vol. 41, pp. A220-A245, 2019.
- [8] M. J. Gander, S. L. Wu. *Convergence analysis of a periodic-like waveform relaxation method for initial-value problems via the diagonalization technique*. Numer. Math., Vol. 143, pp. 489-527, 2019.
- [9] M. J. Gander and S. Vandewalle. *Analysis of the parareal time-parallel time-integration method*, SIAM J. Sci. Comput., Vol. 29, pp. 556-578, 2007.
- [10] J.-L. Lions, Y. Maday, and G. Turinici. *A “parareal” in time discretization of PDE’s*, C. R. Acad. Sci. Paris Sér. I Math., Vol. 332, pp. 661-668, 2001.
- [11] B. Y. Li, J. Liu, and M. Xiao. *A fast and stable preconditioned iterative method for optimal control problem of wave equations*. SIAM J. Sci. Comput., Vol. 37, pp. A2508-A2534, 2015.
- [12] Y. Maday and E. M. Rønquist. *Parallelization in time through tensor-product space-time solvers*. Comptes Rendus Mathématique, Vol. 346, pp. 113-118, 2008.
- [13] E. McDonald, J. Pestana, and A. Wathen. *Preconditioning and iterative solution of all-at-once systems for evolutionary partial differential equations*. SIAM J. Sci. Comput., Vol. 40, pp. A1012-A1033, 2018.
- [14] S. Sahni and V. Thanvantri. *Performance metrics: Keeping the focus on runtime*. IEEE Parall. Distrib., Vol. 4, pp. 43-56, 1996.
- [15] S. L. Wu. *Toward parallel coarse grid correction for the parareal algorithm*. SIAM J. Sci. Comput., Vol. 40, pp. A1446-A1472, 2018.
- [16] S. L. Wu and J. Liu. *A parallel-in-time block-circulant preconditioner for optimal control of wave equations*. SIAM J. Sci. Comput., Vol. 42, pp. A1510-A1540, 2020.
- [17] S. L. Wu and T. Zhou. *Acceleration of the MGRiT algorithm via the diagonalization technique*. SIAM J. Sci. Comput., Vol. 41, pp. A3421-A3448, 2019.
- [18] J. Liu and S. L. Wu. *A fast block α -circulant preconditioner for all-at-once systems from wave equations*. SIAM J. Matrix Anal. Appl., in review.
- [19] X. J. Yang, X. K. Liao, W. X. Xu, J. Q. Song, Q. F. Hu, J. S. Su, L. Q. Xiao, K. Lu, Q. Dou, J. P. Jiang, and C. Q. Yang. *TH-1: China’s first petaflop supercomputer*. Front. Comput. Sci. China, Vol. 4, pp. 445-455, 2010.